J. Cent. South Univ. (2019) 26: 2000−2010
DOI: https://doi.org/10.1007/s11771-019-4147-y

Springer

Navier's slip condition on time dependent Darcy-Forchheimer nanofluid using spectral relaxation method

Younghae DO[1], G. K. RAMESH[2], G. S. ROOPA[3], M. SANKAR[4]

1. Department of Mathematics, KNU-Center for Nonlinear Dynamics, Kyungpook National University, Daegu, 41566, Korea;
2. Department of Mathematics, K.L.E. Society's J.T. College, Gadag-582102, Karnataka, India;
3. Department of Mathematics, Malnad College of Engineering, Hassan-573202, Karnataka, India;
4. Department of Mathematics, School of Engineering, Presidency University, Bengaluru-560064, Karnataka, India

Abstract: In industrial applications involving metal and polymer sheets, the flow situation is strongly unsteady and the sheet temperature is a mixture of prescribed surface temperature and heat flux. Further, a proper choice of cooling liquid is also an important component of the analysis to achieve better outputs. In this paper, we numerically investigate Darcy-Forchheimer nanoliquid flows past an unsteady stretching surface by incorporating various effects, such as the Brownian and thermophoresis effects, Navier's slip condition and convective thermal boundary conditions. To solve the governing equations, using suitable similarity transformations, the nonlinear ordinary differential equations are derived and the resulting coupled momentum and energy equations are numerically solved using the spectral relaxation method. Through the systematically numerical investigation, the important physical parameters of the present model are analyzed. We find that the presence of unsteadiness parameter has significant effects on velocity, temperature, concentration fields, the associated heat and mass transport rates. Also, an increase in inertia coefficient and porosity parameter causes an increase in the velocity at the boundary.

Key words: Darcy-Forchheimer flow; nanoliquid; Navier's slip; convective condition; numerical solution

Cite this article as: Younghae DO, G. K. RAMESH, G. S. ROOPA, M. SANKAR. Navier's slip condition on time dependent Darcy-Forchheimer nanofluid using spectral relaxation method [J]. Journal of Central South University, 2019, 26(7): 2000−2010. DOI: https://doi.org/10.1007/s11771-019-4147-y.

1 Introduction

The rapid growth in electronic industry needs exceptional cooling technique for the modern devices to avoid overheating or hot spot occurrences. Since the conventional working fluids have inadequate cooling capability, the highly demanding cooling requirement by the industry could not be achieved. Therefore, nanoliquids with high thermal conductivities become suitable alternates to the conventional fluids in cooling technology and also play an important role in the enhancement of heat transfer. As a result, many experimental and theoretical investigations on various aspects of heat transfer mechanisms involving nanoliquids have been found in the literature. CHOI et al [1] performed the pioneering experiments and revealed that the thermal conductivity of the liquid can be increased by

Foundation item: Project(NRF-2016R1A2B4011009) supported by National Research Foundation of Korea; Project(KSTePS/VGST-KFIST(L1)/2017) supported by Vision Group of Science and Technology, Government of Karnataka, India
Received date: 2018-05-24; **Accepted date:** 2018-11-02
Corresponding author: G. K. RAMESH, PhD; Tel: +91-9900981204; E-mail: gkrmaths@gmail.com; ORCID: 0000-0001-9404-2823

adding nano-sized particles in the base liquid called as nanoliquid. Later, BUONGIORNO [2] developed a model for convective transport of nanoliquid by taking Brownian diffusion and thermophoresis effects. Using the Buongiorno's model, KHAN et al [3] developed a new mathematical model for boundary layer flow of a nanoliquid due to stretching sheet. Using the model suggested by KHAN et al [3], several investigations have been carried out on the fluid flow and heat transfer from stretching sheet by considering various effects. Among them, the notable studies include NIELD et al [4], MUSTAFA et al [5], BACHOK et al [6], RAMESH et al [7].

Convective flow and associated heat transport through porous medium have important applications in geophysics, heat exchanger design and geothermal energy systems. Also, the applications extend to ground water system, petroleum resources and energy storage unit. When modeling the flow in porous media, Darcy's law is one of the most popular models. However, it is generally recognized that Darcy's model may over-predict the convective flows when inertial drag and vorticity diffusion coefficient are taken into account. The extension of classical Darcy model includes inertial drag and vorticity diffusion. To study the inertial drag and vorticity diffusion, FORCHHEIMER [8] incorporated the square velocity factor. MUSKAT [9] named Forchheimer term and concluded that the inclusion of Forchheimer term is valid for high Reynolds number. PAL et al [10] studied the hydromagnetic Darcy-Forchheimer flow for variable fluid property. Using HAM method, HAYAT et al [11] obtained the analytical solution for Darcy-Forchheimer flow of Maxwell fluid by considering the Cattaneo-Christov theory. VISHNU GANESH et al [12] examined the viscous and ohmic dissipations, and second order slip effects on Darcy–Forchheimer flow of nanoliquid past a stretching/shrinking surface. Mathematical model for Darcy-Forchheimer flow of Maxwell liquid with magnetic field and convective boundary condition are given by ADILSADIQ [13]. Using Keller-box method, ISHAK et al [14] numerically analyzed the magnetohydrodynamic flow and heat transfer performances over a stretching cylinder. Mixed convective flow and the associated heat and mass transfer characteristics over a vertical sheet saturated in a porous medium have been investigated by PAL et al [15] by considering various effects such as Soret, Dufour, thermal radiation and first order chemical reaction. Recently HAYAT et al [16−21] performed detailed analysis in this direction by considering different effects.

The above mentioned investigations are focused only on the flow and thermal analysis for steady state. However, few essential engineering application requires the knowledge of time dependent factor (see MAITY [22], ZHANG et al [23], NAVEED et al [24], OYELAKIN et al [25], MANSUR et al [26, 27]). In the study of micro/nano mechanical systems, the flow behavior does not obey the no-slip boundary condition for cases such as polymer solutions, foams and emulsions. Realizing this important aspect, NAVIER [28] derived a new condition known as velocity slip condition at the solid-liquid interface and it is an important condition in dealing with such fluids. In addition, many heat transfer problems require the implementation of the convective boundary condition due to time dependent flow. AZIZ [29] described the importance of Biot number in the heat transport characteristic. Further, MAKINDE et al [30] examined the convective condition on boundary layer flow of a nanofluid past a stretching sheet. Recently, RAMESH et al [31, 32] reported the applicability of convective boundary condition for flow over a flat plate as well as a stretching sheet.

Based on the careful and thorough literature survey stated above [1−32], it has been found that the effects of unsteadiness and convective thermal boundary conditions on the nanoliquid flow over a stretching sheet have not been attempted in the literature. In spite of the important applications, the combined influences of unsteadiness and convective thermal boundary conditions on Darcy-Forchheimer flow of a nanoliquid over a stretching sheet remains poorly understood in the literature, which motivates the present investigation. In addition, we have also included the uniform heat source/sink, Brownian and thermophoresis effects where the flow is generated due to linear stretched surface. The model equations are numerically solved using spectral relaxation method and the key

parameters are analyzed through graphs and tables. Further, the present results are validated with the existing similar investigations and found good agreement.

The remaining part of the manuscript is structured as follows. The mathematical formulation and model equations for nanoliquid flow is presented in Section 2. In Section 3, numerical methodology and validation are discussed. In Section 4, the detailed analysis of the results is given. Summary and conclusion are presented in Section 5.

2 Mathematical model

The unsteady two-dimensional flow of an electrically conducting nanoliquid is shown in Figure 1. The incompressible Newtonian liquid saturates the porous medium characterizing Darcy-Forchheimer relation. Further, the flow analysis consists of Brownian motion, thermophoresis and uniform heat source/sink. The time dependent uniform magnetic field $B(t)$ is applied along the y− direction. If t is positive, it is assumed that the sheet velocity is $U_{\mathrm{w}}=\dfrac{Hx}{t}$, where H is the positive constant. Further, it is assumed that the sheet surface is heated by a hot liquid having temperature T_{f} and the coefficient of heat transfer is h_{f}.

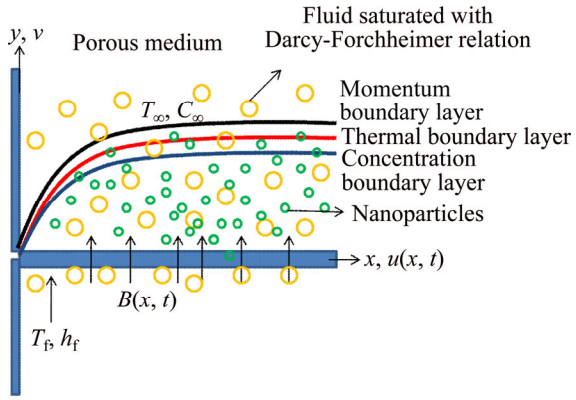

Figure 1 Physical configuration and coordinate system

Employing the above mentioned assumptions, the non-linear partial differential equations governing the unsteady flow of mass, momentum, heat and nanoparticles concentration are (BACHOK et al [6] and VISHNU GANESH et al [12])

$$\frac{\partial u}{\partial x}+\frac{\partial v}{\partial y}=0 \tag{1}$$

$$\frac{\partial u}{\partial t}+u\frac{\partial u}{\partial x}+v\frac{\partial u}{\partial y}=\nu\frac{\partial^2 u}{\partial y^2}-\frac{\sigma B^2(t)}{\rho}u-\frac{\nu}{K(t)}u-Fu^2 \tag{2}$$

$$\frac{\partial T}{\partial t}+u\frac{\partial T}{\partial x}+v\frac{\partial T}{\partial y}=\alpha\frac{\partial^2 T}{\partial y^2}+\frac{\rho_p c_p}{\rho_f c_f}\left[D_{\mathrm{B}}\left(\frac{\partial T}{\partial y}\frac{\partial C}{\partial y}\right)+\frac{D_{\mathrm{T}}}{T_\infty}\left(\frac{\partial T}{\partial y}\right)^2\right]+\frac{Q_0}{\rho_p c_p}(T-T_\infty) \tag{3}$$

$$\frac{\partial C}{\partial t}+u\frac{\partial C}{\partial x}+v\frac{\partial C}{\partial y}=\left[D_{\mathrm{B}}\left(\frac{\partial^2 C}{\partial y^2}\right)+\frac{D_{\mathrm{T}}}{T_\infty}\left(\frac{\partial^2 T}{\partial y^2}\right)\right] \tag{4}$$

where u and v represent the velocity component in the x- and y- direction, respectively. The relevant parameters are the kinematic viscosity ν, the electrical conductivity σ, the density of the base fluid ρ, the time-dependent permeability of the porous medium $K(t)$, the non-uniform inertia coefficient $F=\dfrac{c_b}{xK^{0.5}}$, the drag coefficient c_b, the thermal diffusivity α, the heat capacity of nanoparticles $\rho_p c_p$, the heat capacity of base fluid $\rho_{\mathrm{f}} c_{\mathrm{f}}$, the Brownian diffusivity D_{B}, the thermophoresis diffusivity D_{T}, and the heat generation or absorption coefficient Q_0. The appropriate boundary conditions are

$$\begin{aligned}&t>0,\ u=U_{\mathrm{w}}+U_{\mathrm{slip}},\ -k\frac{\partial T}{\partial y}=-h_{\mathrm{f}}(T_{\mathrm{f}}-T),\\&C=C_{\mathrm{w}}\ \text{ at }\ y=0;\\&u\to 0,\ v\to 0,\ T\to T_\infty,\ C\to C_\infty\ \text{as}\ y\to\infty\end{aligned} \tag{5}$$

where $U_{\mathrm{slip}}=N_1\mu\dfrac{\partial u}{\partial y}$, and N_1, μ and $k=k_0t^{0.5}$ indicate the velocity slip factor, the dynamic viscosity and the thermal conductivity, respectively.

For computational analysis, the partial differential Eqs. (1) to (4) can be converted into ordinary differential equations by using the following similarity variables as suggested by MANSUR and ISHAK [26]:

$$\begin{aligned}&\psi=Ax\left(\frac{\nu}{t}\right)^{0.5}f(\eta),\ \eta=(\nu t)^{-0.5}y,\\&\theta(\eta)=\frac{T-T_\infty}{T_{\mathrm{f}}-T_\infty},\ \phi(\eta)=\frac{C-C_\infty}{C_{\mathrm{f}}-T_\infty}\end{aligned} \tag{6}$$

In the above relation, η and ψ are the similarity variable and the similarity function, respectively, which can be defined by $u=\dfrac{\partial\psi}{\partial y}$, $v=-\dfrac{\partial\psi}{\partial x}$. Further, the variables T, C, T_{f}, C_{f}, T_∞, and C_∞ indicate the temperature of the liquid, the nanoparticles

concentration, the uniform temperature, uniform nanoparticles concentration, the temperature and nanoparticles concentration far from the surface, respectively.

To obtain the dynamical solutions of fluid motion, we chose the velocity slip, time dependent transverse magnetic field and permeability of porous medium as

$$N_1 = N_2\left(\frac{t}{\nu}\right)^{0.5},\ B^2(t) = \frac{B_0^2}{t},\ K(t) = \frac{K}{t} \tag{7}$$

Using Eqs. (6) and (7), we get the following non-dimension velocity, temperature and concentration equations:

$$\frac{\mathrm{d}^3 f}{\mathrm{d}\eta^3} + A\left(f(\eta)\frac{\mathrm{d}^2 f}{\mathrm{d}\eta^2} - \left(\frac{\mathrm{d}f}{\mathrm{d}\eta}\right)^2\right) + \frac{\eta}{2}\frac{\mathrm{d}^2 f}{\mathrm{d}\eta^2} + \frac{\mathrm{d}f}{\mathrm{d}\eta}\left(1 - M^2 - \lambda\right) - FrA\left(\frac{\mathrm{d}f}{\mathrm{d}\eta}\right)^2 = 0 \tag{8}$$

$$\frac{1}{Pr}\frac{\mathrm{d}^2\theta}{\mathrm{d}\eta^2} + \left(Af(\eta) + \frac{\eta}{2}\right)\frac{\mathrm{d}\theta}{\mathrm{d}\eta} + Nb\frac{\mathrm{d}\theta}{\mathrm{d}\eta}\frac{\mathrm{d}\phi}{\mathrm{d}\eta} + Nt\left(\frac{\mathrm{d}\theta}{\mathrm{d}\eta}\right)^2 + Q\theta(\eta) = 0 \tag{9}$$

$$\frac{\mathrm{d}^2\phi}{\mathrm{d}\eta^2} + \frac{Nb}{Nt}\frac{\mathrm{d}^2\theta}{\mathrm{d}\eta^2} + Le\left(Af(\eta) + \frac{\eta}{2}\right)\frac{\mathrm{d}\phi}{\mathrm{d}\eta} = 0 \tag{10}$$

Also, the boundary conditions, given in Eq. (5), reduce to the following form:

$$f(\eta) = 0,\ \frac{\mathrm{d}f}{\mathrm{d}\eta} = 1 + \delta\frac{\mathrm{d}^2 f}{\mathrm{d}\eta^2},\ \frac{\mathrm{d}\theta}{\mathrm{d}\eta} = -Bi(1 - \theta(\eta)),$$
$$\phi(\eta) = 1 \ \text{ at } \eta = 0;$$
$$\frac{\mathrm{d}f}{\mathrm{d}\eta} \to 0,\ \theta(\eta) \to 0,\ \phi(\eta) \to 0 \ \text{ as } \ \eta \to \infty \tag{11}$$

The dimensionless parameters appearing in this analysis are the unsteady term A, the magnetic parameter M, the porosity parameter λ, the inertia coefficient Fr, the Prandtl number Pr, the Brownian motion parameter Nb, the thermoporosis parameter Nt, the heat source (Q>0) or heat sink (Q<0), the Lewis number Le, the velocity slip parameter δ, and the Biot number Bi, which are defined as

$$M = \frac{\sigma B_0^2}{\rho},\ \lambda = \frac{\nu}{K},\ Fr = \frac{C_\mathrm{b}}{K^{0.5}},\ Pr = \frac{\nu}{\alpha},$$
$$Nb = \frac{\rho_p c_p}{\nu\rho_\mathrm{f} c_\mathrm{f}} D_\mathrm{B}(C_\mathrm{f} - C_\infty),\ Nt = \frac{\rho_p c_p}{\nu T_\infty \rho_\mathrm{f} c_\mathrm{f}} D_\mathrm{T}(T_\mathrm{f} - T_\infty),$$
$$Q = \frac{Q_0}{\rho_p c_p},\ Le = \frac{\alpha}{D_\mathrm{B}},\ \delta = N_2\rho,\ Bi = \frac{h_\mathrm{f}\nu^{0.5}}{k_0}.$$

The physical expression for the skin friction coefficient C_f, the local Nusselt number Nu and the local Sherwood number Sh can be defined as

$$C_\mathrm{f} = \frac{\tau_\mathrm{w}}{\rho U_\mathrm{w}^2},\ Nu = \frac{xq_\mathrm{w}}{k(T_\mathrm{f} - T_\infty)},\ Sh = \frac{xq_\mathrm{m}}{D_\mathrm{B}(C_\mathrm{w} - C_\infty)}$$

where the surface shear stress τ_w, surface heat flux q_w and surface mass flux q_w can be defined in the following expressions:

$$\tau_\mathrm{w} = \mu\left(\frac{\partial u}{\partial y}\right)_{y=0},\ q_\mathrm{w} = -k\left(\frac{\partial T}{\partial y}\right)_{y=0},$$
$$q_\mathrm{m} = -D_\mathrm{B}\left(\frac{\partial C}{\partial y}\right)_{y=0}.$$

After applying the similarity transformations given in Eq. (6), the following dimensionless expressions for skin friction, local Nusselt and Sherwood numbers are obtained:

$$C_\mathrm{f} Re_x^{1/2} = -Af''(0),\ NuRe_x^{-1/2} = -A\theta'(0),$$
$$ShRe_x^{-1/2} = -A\phi'(0)$$

where $Re_x = \dfrac{U_\mathrm{w} x}{\nu}$ is the Reynolds number.

In the absence of the parameters M, λ, Fr, δ, Q, Bi and A, the present system of governing Eqs. (8) to (11) reduces to those of KHAN and POP [3]. Also in the absence of magnetic field, heat source/sink, slip parameter, porosity parameter and inertial coefficient, the present model equations reduce to those of MANSUR and ISHAK [26]. Hence, in the absence of Darcy-Forchheimer relation and Navier's slip condition, the boundary layer flow and energy transform regular nanoliquid problem degenerate. For this analysis, numerical simulation for velocity, temperature and concentration curves is obtained.

3 Numerical method and validation

The governing Eqs. (8) to (10) are highly non-linear and coupled ordinary differential equations and hence it is not amenable to analytical solution. Therefore, the governing ordinary differential equations are solved using spectral relaxation method. To apply this method, first we set $\dfrac{\mathrm{d}f}{\mathrm{d}\eta} = f' = g$ and the governing Eqs. (8) to (10) reduce to

$$f' = g,$$

$$g''+A[fg'-g^2]+\frac{\eta}{2}g'+g[1-M^2-\lambda]-AFrg^2=0,$$
$$\frac{\theta''}{Pr}+\left(Af+\frac{\eta}{2}\right)\theta'+Nb\theta'\phi'+Nt(\theta')^2+Q\theta=0,$$
$$\phi''+\frac{Nb}{Nt}\theta''+Le\left(Af+\frac{\eta}{2}\right)\phi'=0.$$

Also, the corresponding initial and boundary conditions become

$$f(0)=0,\ g(0)=1+\delta g'(0),\ \theta'(0)=-Bi(1-\theta(0)),$$
$$\phi(0)=1,\ g(\infty)\to 0,\ \theta(\infty)\to 0,\ \phi(\infty)\to 0.$$

The spectral relaxation iteration procedure for the present problem can be written as

$$f'_{r+1}=g_r,$$
$$g''_{r+1}+\left(Af_{r+1}+\frac{\eta}{2}\right)g'_{r+1}+\left(1-M^2-\lambda\right)g_{r+1}=A(Fr+1)g_r^2,$$
$$\frac{\theta''_{r+1}}{Pr}+\left(Af_{r+1}+\frac{\eta}{2}+Nb\phi'\right)\theta'_{r+1}+Q\theta_{r+1}=-Nt\left(\theta'_r\right)^2,$$
$$\phi''_{r+1}+Le\left(Af_{r+1}+\frac{\eta}{2}\right)\phi'_{r+1}=-\frac{Nb}{Nt}\theta''_{r+1},$$
$$f_{r+1}(0)=0,\ g_{r+1}(0)=1+\delta g'_{r+1}(0),$$
$$\theta'_{r+1}(0)=-Bi(1-\theta_{r+1}(0)),\ \phi_{r+1}(0)=1,$$
$$g_{r+1}(\infty)\to 0,\ \theta_{r+1}(\infty)\to 0,\ \phi_{r+1}(\infty)\to 0.$$

Since η varies from η_0 to η_∞, let $\xi=\frac{2\eta}{\eta_\infty}-1$ be the domain mapped into the interval [1, −1] and grid points are defined as $\xi_j=\cos\left(\frac{\pi j}{N}\right)$, where N represents the number of grid points and j=1, 2, 3, ⋯, N. Now applying the Chebyshev pseudo-spectral method to the above equations, the following iterative equations are obtained:

$$P_1f_{r+1}=E_1,\ f_{r+1}(\xi_N)=0,$$
$$P_2g_{r+1}=E_2,\ g_{r+1}(\xi_N)=1+\delta g'_{r+1}(\xi_N),\ g_{r+1}(\xi_0)=0,$$
$$P_3\theta_{r+1}=E_3,\ \theta'_{r+1}(\xi_N)=-Bi(1-\theta_{r+1}(\xi_N)),$$
$$\theta_{r+1}(\xi_0)=0,$$
$$P_4\phi_{r+1}=E_4,\ \phi_{r+1}(\xi_N)=1,\ \phi_{r+1}(\xi_0)=0,$$

where $P_1=D,\ E_1=g_r,$

$$P_2=D^2+\mathrm{diag}\left(Af_{r+1}+\frac{\eta}{2}\right)D+(1-M^2-\lambda)I,$$
$$E_2=Ag_r^2(Fr+1),$$
$$P_3=\frac{D^2}{Pr}+\mathrm{diag}\left(Af_{r+1}+\frac{\eta}{2}+Nb\phi'_r\right)D+QI,$$
$$E_3=-Nt\theta'^2_r,$$
$$P_4=D^2+Le\,\mathrm{diag}\left(Af_{r+1}+\frac{\eta}{2}\right)D,\ E_4=-\frac{Nb}{Nt}\theta''_{r+1}.$$

In the above expressions, I and D represent the identity and the differentiation matrix. The above matrix system of equations are solved iteratively with proper initial guesses of $f_0(\eta)$, $g_0(\eta)$, $\theta_0(\eta)$ and $\phi_0(\eta)$. To solve these equations, an in-house code has been developed in MATLAB program, and is successfully validated with the standard benchmark solutions before obtaining the simulations.

For the validation of present numerical results, the local Nusselt numbers are obtained for different values of Nb and Le in the absence of Fr, δ, λ and Q and are compared with the results of MANSUR et al [27]. An examination of the local Nusselt number, $-\theta'(0)$, between the present simulation and that of MANSUR et al [27], exhibited in Table 1, demonstrates an excellent comparison and accordingly gives confidence that the present numerical outcomes are precise and accurate.

Table 1 Comparison of present local Nusselt number $-\theta'(0)$ with that of MANSUR et al [27] in the absence of Fr, δ, λ, Q with A=1, Pr=6.8

Nb	Le	$-\theta'(0)$	
		MANSUR et al [27]	Present
0.1	2	0.094966	0.0949663
0.3	2	0.091650	0.0916500
0.5	2	0.084814	0.0848135
0.5	3	0.079753	0.0797533
0.5	5	0.071002	0.0710020
0.5	10	0.056647	0.0566468

4 Results and discussion

In this section, the salient features of the flow, heat and mass transfer rates are discussed elaborately for various parameters of the study. The present analysis consists of eleven parameters, namely unsteady parameter (A), magnetic parameter (M), porosity parameter (λ), inertia coefficient (Fr), Prandtl number (Pr), Brownian motion parameter (Nb), thermoporosis parameter (Nt), heat source/sink parameter (Q), Lewis number (Le), velocity slip parameter (δ) and Biot number (Bi). The qualitative as well as quantitative effects of each of these parameters are obtained through the systematic numerical simulations. In particular, the influences of the above parameters on velocity,

temperature and concentration profiles are analyzed. However, the quantitative variations, such as skin friction ($f''(0)$), heat transfer ($\theta'(0)$) and mass transfer ($\phi'(0)$) with respect to the above parameter combinations are discussed through Table 2.

Figure 2 exhibits the effects of velocity slip parameter on the velocity field by fixing other parameters. It reveals that larger value of slip parameter (δ) corresponds to reduction in the velocity field. Physically, it can be interpreted that, for higher values of δ, the resistance between the nanoliquid and sheet gets diminished and nanoliquid acts like inviscid liquid which leads to a complete slip. It is important to mention that the consideration of slip condition is more appropriate for the kind of fluids considered in the analysis and no-slip condition may lead to physically incorrect results.

Table 2 Values of $-f''(0)$, $-\theta'(0)$ and $-\phi'(0)$ for different governing physical parameters

Parameter		$-f''(0)$	$-\theta'(0)$	$-\phi'(0)$
A	0.0	0.580563935	0.295802097	0.213306347
	0.2	0.587391995	0.303092279	0.215707487
	0.4	0.593629371	0.309459234	0.218648867
Bi	0.2	0.587391995	0.159591136	0.306859697
	0.5	0.587391995	0.303092279	0.215707487
	0.8	0.587391995	0.388995578	0.162281069
Fr	0.3	0.586754092	0.303108189	0.215717591
	0.5	0.587391995	0.303092279	0.215707487
	0.7	0.588024463	0.303076509	0.215697488
λ	0.0	0.561338061	0.303830280	0.216410663
	0.2	0.575083816	0.303439545	0.216028570
	0.4	0.587391995	0.303092279	0.215707487
δ	0.0	1.477882010	0.312231341	0.220200233
	0.5	0.837016964	0.305857396	0.216882451
	1.0	0.587391995	0.303092279	0.215707487
Nb	0.1	0.587391995	0.313630077	0.008817670
	0.2	0.587391995	0.303092279	0.215707487
	0.3	0.587391995	0.291837709	0.291135452
Nt	0.1	0.587391995	0.306317715	0.310997570
	0.2	0.587391995	0.303092279	0.215707487
	0.3	0.587391995	0.299711455	0.125168928
Le	0.5	0.587391995	0.303092279	0.215707487
	1.0	0.587391995	0.293570624	0.430871666
	2.0	0.587391995	0.282363450	0.725232271
Pr	1.0	0.587391995	0.246272925	0.279301733
	2.0	0.587391995	0.283218656	0.239188326
	3.0	0.587391995	0.303092279	0.215707487
Q	−0.05	0.587391995	0.303092279	0.215707487
	0.0	0.587391995	0.313589975	0.200774963
	0.05	0.587391995	0.322556164	0.187977845
M	1.0	0.476537547	0.306284022	0.219295496
	1.5	0.587391995	0.303092279	0.215707487
	2.0	0.659449775	0.301127133	0.214226219

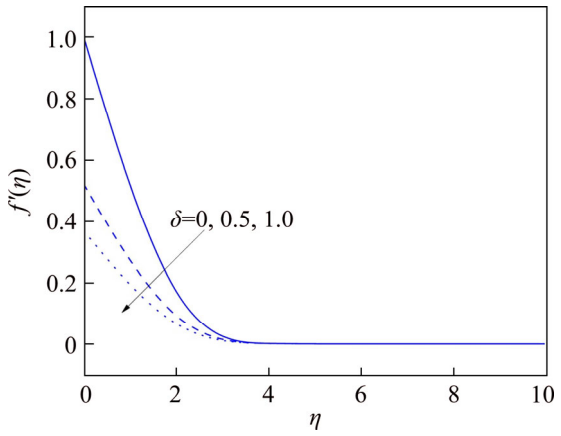

Figure 2 Effects of δ on velocity profiles f'

The influence of time-dependent parameter on velocity, temperature and concentration fields is displayed in Figure 3. A careful observation of the result reveals that higher values of unsteadiness parameter reduce the fluid velocity. Physically, it can be interpreted that the velocity of liquid along the sheet diminishes with an expansion in the unsteadiness parameter due to decrease in the thickness of the momentum boundary layer.

Also, the thermal and solutal profiles demonstrate that the temperature and concentration profiles diminish significantly as the unsteadiness

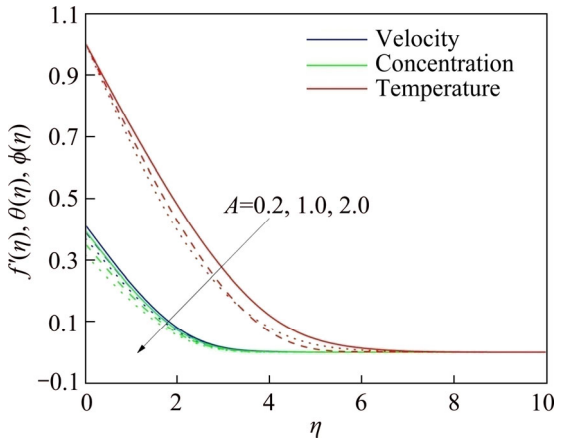

Figure 3 Effects of A on velocity, temperature and concentration profiles f', θ, ϕ

parameter increases. The rate of heat transfer (from the sheet to the liquid) diminishes with expanding estimations of A. It is observed that less heat is exchanged from the sheet to the liquid when the unsteadiness parameter increases and consequently, the temperature profiles $\theta(\eta)$ diminishes. Since the liquid flow is caused exclusively by the extending sheet and the sheet surface temperature is higher than the free stream temperature, the liquid velocity and temperature diminish as A increases. Note that the rate of cooling with higher values of unsteadiness parameter is significantly faster than that with lower unsteadiness parameter values.

Figure 4 represents the variation of porosity parameter on velocity profiles. A general observation of Figure 4 reveals that as λ increases, the velocity and related boundary layer thickness decrease. This is due to the resistive force employed by the porous medium. For large porousness, i.e. for diminishing λ, the liquid gets more space to flow and as a result the velocity augments. However, the change in velocity is the maximum for close to the surface and far from the surface, and this change is little or zero. The nearness of the permeable medium makes higher confinement for the liquid, which decreases the liquid velocity. The momentum layer thickness diminishes when λ increases.

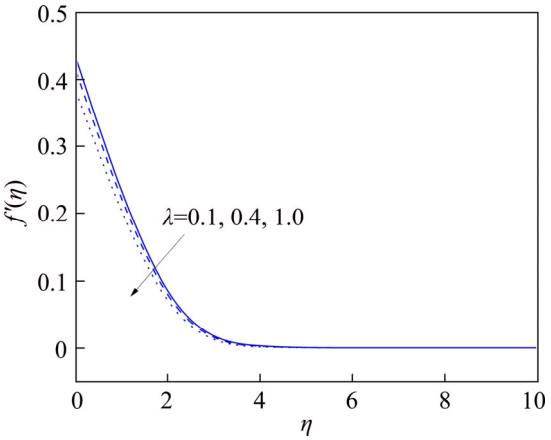

Figure 4 Effects of λ on velocity profiles f'

Figures 5 and 6 are presented to analyze the behavior of temperature profiles with respect to Biot number and heat source/sink parameter. Figure 5 demonstrates that the surface temperature increases with an increase in Biot number. It is noted that for higher values of Biot number, convective heating increases and isothermal surface (i.e. $\theta(0)=1$) is reproduced as $Bi\to\infty$. Physically, this indicates that larger values of Biot number raise the resistance of the internal thermal surface than the resistance of boundary layer surface. The variation of temperature profiles for distinct values of heat source/sink parameter is displayed in Figure 6. From the figure, it is observed that the thermal boundary layer generates the energy and this causes the temperature increases with an increase of heat source parameter, whereas an opposite result can be found for heat sink parameter. For Q is positive value (heat source), it can be noted that the thermal layer produces energy and this causes the temperature in the thermal layer increases with an increment in Q. However, the negative value of Q (heat sink) prompts a diminish in the thermal layer. Also, Q is zero, indicating that there is non-appearance of heat source/sink parameter.

Figure 7 displays the effect of Brownian motion and thermoporosis parameter on temperature and concentration fields. It reveals that increasing Nb and Nt simultaneously, the thickness of the thermal and solutal boundary layer is

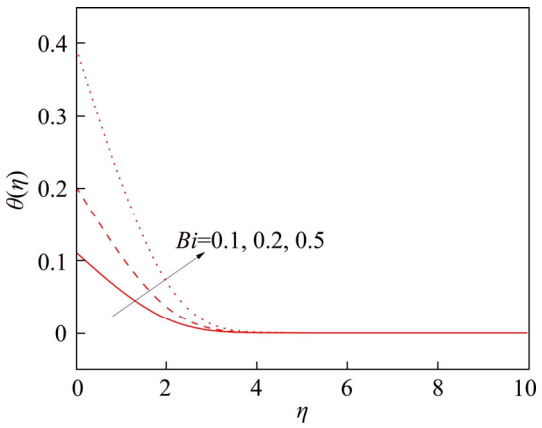

Figure 5 Effects of Bi on temperature profiles θ

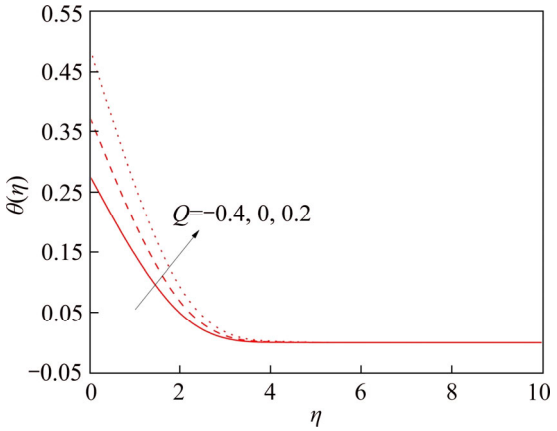

Figure 6 Effects of Q on temperature profiles θ

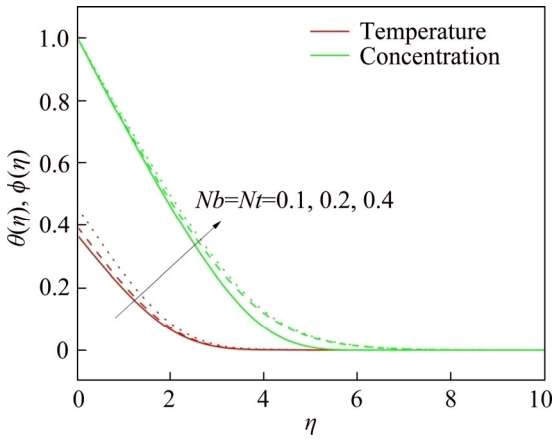

Figure 7 Effects of *Nb*, *Nt* on temperature and concentration profiles θ, ϕ

enhanced. The part of thermophoretic force is with the end goal that the nanoparticles close to the hot boundary are being pushed towards the cold liquid at the ambient. Accordingly, it can be anticipated that the thermal layer will end up noticeably thicker in the nearness of thermophoretic impact.

Figures 8 and 9 demonstrate the effects of Lewis number, Brownian motion parameter and thermoporosis parameter on concentration fields. The effect of Lewis number on concentration distribution is presented in Figure 8. From the definition, Lewis number is dependent on Brownian diffusion coefficient. As regards to the influence of Lewis number, it has been noted that larger values of Lewis number waken the Brownian diffusion coefficient, which in turn reduces the concentration level. Further, from Figure 7, it is witnessed that concentration distribution is accelerating function of both Brownian motion parameter and thermoporosis parameter.

The variation of $-f''(0)$ with respect to M, for

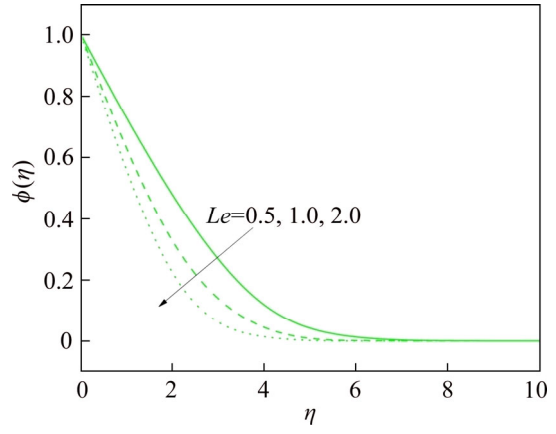

Figure 8 Effects of *Le* on concentration profiles ϕ

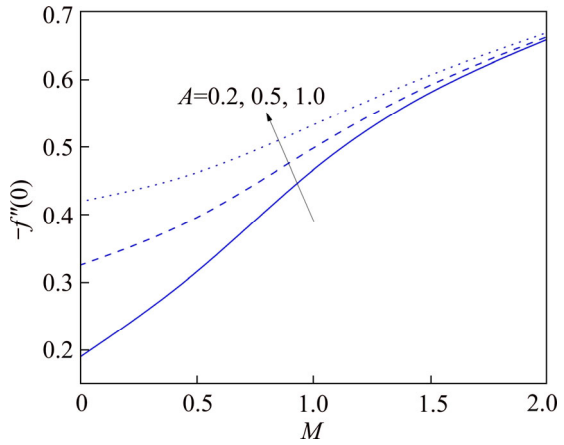

Figure 9 Variation of M and $-f''(0)$ with A

distinct values of A is depicted in Figure 9. An increase in the unsteadiness parameter, A, leads to enhancing the $-f''(0)$. It is observed that for different values of M, we get negative values of $f''(0)$. Negative value indicates that surface exerts a drag force on the liquid and this happens when the sheet is stretching. Similar phenomenon can be observed for the variation of $-f''(0)$ with respect to A, for distinct values of Fr, λ displayed in Figure 10. The variations of friction factor, Nusselt and Sherwood numbers with different physical parameters are displayed in Table 2.

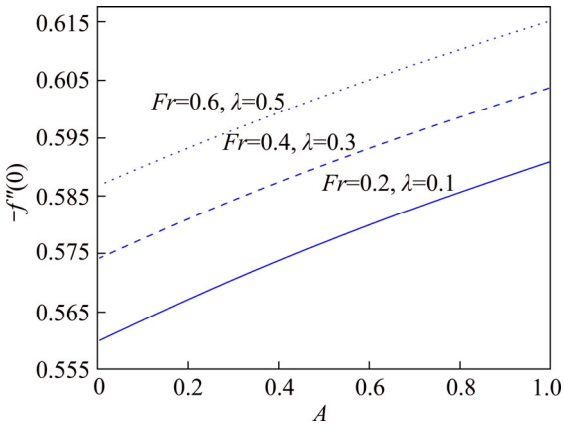

Figure 10 Variation of A and $-f''(0)$ with Fr, λ

It is noted that skin friction increases with A, Fr, λ and decreases with δ, M. Further, we observed the increase of Bi, Nb, Nt, Le, Pr and Q have no variation in $-f''(0)$, which is in good agreement with Eq. (8). From this table, we also noted that the local Nusselt number reduces for Fr, λ, δ, Nb, Nt, Le, M and enhances for A, Bi, Pr, Q. The same observation can be noted for local Sherwood number except for Bi, Nb, Pr, Q.

5 Conclusions

The present study analyzes the unsteady Darcy-Forchheimer flow of nanoliquid past an unsteady stretching surface in the presence of porous medium, magnetic field and heat source/sink parameter. Based on the detailed numerical simulations, the following conclusions are obtained.

The unsteadiness parameter has a strong role in controlling the flow pattern, thermal and concentration distributions. An increase in unsteadiness parameter decays the velocity, temperature and concentration distribution of the flow. Friction factor can be enhanced for larger values of the inertia coefficient and porosity parameter. The thickness of momentum boundary layer decreases due to the increase of velocity slip parameter. The fluid temperature profile increases rapidly as the Biot number increases. Simultaneous increase in the Brownian motion and thermoporosis parameters enhanced both temperature and concentration profiles. At larger values of Lewis number, the concentration distribution reduces. For negative value of Q, the temperature profile decreases and this reveals that heat sink parameter is superior for cooling of the stretching sheet.

The present study made a pioneering attempt to analyze the important effects of unsteadiness, Navier slip and convective thermal boundary conditions on the nanoliquid flow over a stretching sheet. The results of present study can be utilized in establishing a basic understanding of these effects in the industrial applications that include both metal and polymer sheets.

Nomenclature

A Unsteadiness parameter
$B(t)$ Time-dependent uniform magnetic field, kg/(s^2·A)
Bi Biot number
C_f Skin friction
c_p Specific heat, m^2/s^2
C Nanoparticle volume fraction, kg/m^3
D_B Brownian diffusion coefficient, m^2/s
D_T Thermophoresis diffusion coefficient, m^2/s
F Non-uniform inertia coefficient
Fr Inertia coefficient
$K(t)$ Time-dependent permeability of porous medium
M Magnetic parameter
N_1 Velocity slip factor, m
Nb Brownian motion parameter
Nt Thermophoresis parameter
Nu Local Nusselt number
Le Lewis number
Pr Prandtl number
Q_0 Heat generation/absorption coefficient
Q Heat source/sink parameter
Sh Local Sherwood number
t Time, s
T Temperature of fluid, K
T_w Temperature at wall, K
T_∞ Ambient fluid temperature, K
u, v Velocity components along x- and y-directions, m/s

Greek symbols

U_w Sheet velocity
ν Kinematic viscosity, m^2/s
ϕ Dimensionless concentration
ρ_f Density of the base fluid, kg/s^3
λ Porosity parameter
δ Velocity slip parameter
θ Dimensionless temperature
η Similarity variable
α Thermal diffusivity, m^2/s
τ_w Wall shearing stress, kg/(m·s^2)

References

[1] CHOI S, EASTMAN J A. Enhancing thermal conductivity of fluids with nanoparticles [J]. ASME-Publ Fed, 1995, 231: 99−106.

[2] BUONGIORNO J. Convective transport in nanofluids [J]. J Heat Trans, 2006, 128(3): 240−250. DOI: 10.1115/1.2150834.

[3] KHAN W A, POP I. Boundary-layer flow of a nanofluid past a stretching sheet [J]. International Journal of Heat and Mass Transfer, 2010, 53(11, 12): 2477−2483. DOI: 10.1016/ j.ijheatmasstransfer.2010.01.032.

[4] NIELD D A, KUZNETSOV A V. The Cheng–Minkowycz problem for natural convective boundary-layer flow in a porous medium saturated by a nanofluid [J]. International Journal of Heat and Mass Transfer, 2009, 52(25, 26): 5792−5795. DOI: 10.1016/ j.ijheatmasstransfer.2009.07.024.

[5] MUSTAFA M, HAYAT T, POP I, ASGHAR S, OBAIDAT S. Stagnation-point flow of a nanofluid towards a stretching

sheet [J]. International Journal of Heat and Mass Transfer, 2011, 54(25, 26): 5588−5594. DOI: 10.1016/ j.ijheatmasstransfer.2011.07.021.

[6] BACHOK N, ISHAK A, POP I. Unsteady boundary-layer flow and heat transfer of a nanofluid over a permeable stretching/shrinking sheet [J]. International Journal of Heat and Mass Transfer, 2012, 55(7, 8): 2102−2109. DOI: 10.1016/ j.ijheatmasstransfer.2011.12.013.

[7] RAMESH G K, PRASANNAKUMARA B C, GIREESHA B J, SHEHZAD S A, ABBASI F M. Three dimensional flow of Maxwell fluid with suspended nanoparticles past a bidirectional porous stretching surface with thermal radiation [J]. Thermal Science and Engineering Progress, 2017, 1: 6−14. DOI: 10.1016/j.tsep.2017.02.006.

[8] FORCHHEIMER P. Wasserbewegung durch boden [J].Zeit Ver Deut Ing, 1901, 45: 1782−1788.

[9] MUSKAT M. The flow of homogeneous fluids through porous media [M]. New York: McGraw-Hill Book Company, 1937.

[10] PAL D, MONDAL H. Hydromagnetic convective diffusion of species in Darcy-Forchheimer porous medium with non-uniform heat source/sink and variable viscosity [J]. Int Com Heat Mass Transfer, 2012, 39(7): 913−917. DOI: 10.1016/j.icheatmasstransfer.2012.05.012.

[11] HAYAT T, MUHAMMAD T, Al-MEZAL S, LIAO S J. Darcy-Forchheimer flow with variable thermal conductivity and Cattaneo-Christov heat flux [J]. Int J Numer Methods Heat Fluid Flow, 2016, 26(8): 2355−2369. DOI: 10.1108/HFF-08-2015-0333.

[12] VISHNU GANESH N, ABDUL HAKEEM A K, GANGA B. Darcy–Forchheimer flow of hydromagnetic nanofluid over a stretching/shrinking sheet in a thermally stratified porous medium with second order slip, viscous and Ohmic dissipations effects [J]. Ain Shams Engineering Journal, 2018, 9(4): 939−951. DOI: 10.1016/j.asej.2016.04.019.

[13] ADIL SADIQ M, HAYAT T. Darcy-Forchheimer flow of magneto Maxwell liquid bounded by convectively heated sheet [J]. Results in Physics, 2016, 6: 884−890. DOI: 10.1016/j.rinp.2016.10.019.

[14] ISHAK A, NAZAR R, POP I. Magnetohydrodynamic (MHD) flow and heat transfer due to a stretching cylinder [J]. Energy Conversion and Management, 2008, 49(11): 3265−3269. DOI: 10.1016/j.enconman.2007.11.013.

[15] PAL D, MONDAL H. Influence of chemical reaction and thermal radiation on mixed convection heat and mass transfer over a stretching sheet in Darcian porous medium with Soret and Dufour effects [J]. Energy Conversion and Management, 2012, 62: 102−108. DOI: 10.1016/j.enconman.2012.03.017.

[16] HAYAT T, MUHAMMAD T, SHEHZAD S A, ALSAEDI A. An analytical solution for magnetohydrodynamic Oldroyd-B nanofluid flow induced by a stretching sheet with heat generation/absorption [J]. International Journal of Thermal Sciences, 2017, 111: 274−288. DOI: 10.1016/ j.ijthermalsci.2016.08.009.

[17] HAYAT T, AZIZ A, MUHAMMAD T, ALSAEDI A. On magnetohydrodynamic three-dimensional flow of nanofluid over a convectively heated nonlinear stretching surface [J]. International Journal of Heat and Mass Transfer, 2016, 100: 566−572. DOI: 10.1016/j.ijheatmasstransfer.2016.04.113.

[18] MUHAMMAD T, ALSAEDI A, SHEHZAD S A, HAYAT T. A revised model for Darcy-Forchheimer flow of Maxwell nanofluid subject to convective boundary condition [J]. Chinese Journal of Physics, 2017, 55(3): 963−976. DOI: 10.1016/j.cjph.2017.03.006.

[19] MUHAMMAD T, ALSAEDI A, HAYAT T, SHEHZAD S A. A revised model for Darcy-Forchheimer three-dimensional flow of nanofluid subject to convective boundary condition [J]. Results in Physics, 2017, 7: 2791−2797. DOI: 10.1016/j.rinp.2017.07.052.

[20] HAYAT T, HAIDER F, MUHAMMAD T, ALSAEDI A. On Darcy-Forchheimer flow of viscoelastic nanofluids: A comparative study [J]. Journal of Molecular Liquids, 2017, 233: 278−287. DOI: 10.1016/j.molliq.2017.03.035.

[21] HAYAT T, AZIZ A, MUHAMMAD T, ALSAEDI A. Darcy–forchheimer three-dimensional flow of williamson nanofluid over a convectively heated nonlinear stretching surface [J]. Commun Theor Phys, 2017, 68: 387. DOI: 10.1088/0253-6102/68/3/387.

[22] MAITY S. Unsteady flow of thin nanoliquid film over a stretching sheet in the presence of thermal radiation [J]. The European Physical Journal Plus, 2016, 131: 49. DOI: 10.1140/epjp/i2016-16049-y.

[23] ZHANG Yan, ZHANG Min, BAI Yu. Unsteady flow and heat transfer of power-law nanofluid thin film over a stretching sheet with variable magnetic field and power-law velocity slip effect [J]. Journal of the Taiwan Institute of Chemical Engineers, 2017, 70: 104−110. DOI: 10.1016/j.jtice. 2016.10.052.

[24] NAVEED M, ABBAS Z, SAJID M. Hydromagnetic flow over an unsteady curved stretching surface [J]. Engineering Science and Technology, an International Journal, 2016, 19(2): 841−845. DOI: 10.1016/j.jestch.2015.11.009.

[25] OYELAKIN I S, MONDAL S, SIBANDA P. Unsteady Casson nanofluid flow over a stretching sheet with thermal radiation, convective and slip boundary conditions [J]. Alexandria Engineering Journal, 2016, 55(2): 1025−1035. DOI: 10.1016/j.aej.2016.03.003.

[26] MANSUR S, ISHAK A. Unsteady boundary layer flow of a nanofluid over a stretching/shrinking sheet with a convective boundary condition [J]. Journal of the Egyptian Mathematical Society, 2016, 24(4): 650−655. DOI: 10.1016/ j.joems.2015.11.004.

[27] MANSUR S, ISHAK A. Unsteady boundary layer flow and heat transfer over a stretching sheet with a convective boundary condition in a nanofluid [C]// AIP Conference Proceedings. Kuala Lumpur, Malaysia: AIP Publishing LLC, 2014, 1602: 311−316. DOI: 10.1063/1.4882504.

[28] NAVIER C L M H. Mémoiresur les lois du mouvement des fluids [J]. Mem Acad Sci Inst de France, 1823, 6: 389−440.

[29] AZIZ A. A similarity solution for laminar thermal boundary layer over a flat plate with a convective surface boundary condition [J]. Commun Nonlinear Sci Numer Simul, 2009, 14(4): 1064−1068. DOI: 10.1016/j.cnsns.2008.05.003.

[30] MAKINDE O D, AZIZ A. Boundary layer flow of a nanofluid past a stretching sheet with a convective boundary condition [J]. Int J Therm Sci, 2011, 50(7): 1326−1332. DOI: 10.1016/j.ijthermalsci.2011.02.019.

[31] RAMESH G K, CHAMKHA A J, GIREESHA B J. Boundary layer flow past an inclined stationary/moving flat plate with convective boundary condition [J]. Afrika Matematika, 2016, 27(1, 2): 87−95. DOI: 10.1007/s13370-015-0323-x.

[32] RAMESH G K, GIREESHA B J, GORLA R S R. Boundary layer flow past a stretching sheet with fluid-particle suspension and convective boundary condition [J]. Heat and Mass Transfer, 2015, 51(8): 1061−1066. DOI: 10.1007/s00231-014-1477-z

(Edited by ZHENG Yu-tong)

中文导读

谱松弛法研究时变 Darcy-Forchheimer 流体的 Navier 滑动条件

摘要：在金属和聚合物薄片的工业应用中，流动情况非常不稳定，并且薄片温度由设定的表面温度和热通量共同决定。此外，合理选择冷却液对实验结果也十分重要。本研究中，结合了各种效应(如布朗效应、热泳效应、Navier 滑动条件和对流边界条件)，对流过不稳定拉伸片表面的 Darcy-Forchheimer 流体进行了数值分析。为了求解控制方程，使用了适当的相似变换，导出了非线性常微分方程，并使用谱松弛法对得到的耦合动量和能量方程进行了数值求解。通过系统的数值求解，分析了现有模型中的重要物理参数。发现不稳定参数的存在对速度、温度和浓度场以及相关的热量和质量传输速率具有显着影响。同时，增大惯性系数和孔隙率可加快边界处的速度。

关键词：Darcy-Forchheimer 流体；纳米流体；Navier 滑动；对流边界条件；数值解